An Approximate Model for Determining the Resistance of a Hemispherical Ground Electrode Placed on a Non-homogeneous Truncated Cone

Dragan Vuckovic[1], Dejan Jovanovic[1], Nenad Cvetkovic[1], Dragan Tasic[1], Karolina Kasas-Lazetic[2]

[1] University of Nis, Faculty of electronic engineering, A. Medvedeva 14, 18000 Nis, Serbia; dragan.vuckovic@elfak.ni.ac.rs; dejan.jovanovic@elfak.ni.ac.rs; nenad.cvetkovic@elfak.ni.ac.rs; dragan.tasic@elfak.ni.ac.rs

[2] University of Novi Sad, Faculty of technical sciences, Trg Dositeja Obradovica 6, 21 000 Novi Sad, Serbia; kkasas@uns.ac.rs

Abstract: In this paper we present an approximate analytically oriented approach for determining the resistance of a hemi-spherically-shaped ground electrode placed on the top of a mountain. The mountain is modelled as a non-homogeneous truncated cone consisting of two homogeneous domains with different specific conductivities values. The given procedure extends the existing, previously proposed procedure in which the mountain was modelled as a homogeneous truncated cone. The procedure, proposed in this paper, includes application of the Estimation method, based on idea of finding arithmetic mean of maximal and minimal resistance value. The obtained results are validated and compared with those obtained using the COMSOL program package, based on the finite element method.

Keywords: Estimation method; grounding system; non-homogeneous soil; resistance; hemispherical electrode

1 Introduction

The resistance of the grounding electrode is its most important characteristic and therefore it is of the utmost importance to develop methods for its estimation. This value is influenced by electrode geometry, conductor characteristics, soil structure related to the specific conductivity structure and physical shape of the surrounding ground. The approach of modelling ground as homogeneous half space of flat ground has been used a decades ago [1-2]. The similar is with the procedures which include non-homogeneous ground modeled as multi-layered [3-4], sectoral

[5], semi-spherically [6-7] or semi-cillindrically shaped domain [8]. All these approaches include using of various appropriate numerical methods [9-14]. Very often, facilities having grounding systems as a necessary part are placed at mountains or hills (e.g. antenna towers, wind turbines, etc.) [15-19]. Usually, those terrains are of low specific conductivity. Research dealing with the problem of characterization of grounding systems installed in such places is not so common. An interesting procedure for analysis of a hemispherical ground electrode placed at the top of a hill is proposed in [20]. It is based on the idea of approximating a mountain with a homogeneous truncated cone, while the hemispherical electrode surface is modelled as calotte. These assumptions allow generating approximate analytical expression for the resistance value. In [21], the above-mentioned procedure is improved by assuming current density distribution in two different forms, depending on the observed domain. In this paper, an extension of the approach from [21] is proposed. It offers the possibility of modelling a hill as a non-homogeneous domain consisting of two homogeneous areas, each having different electrical characteristics. The Estimation method application [8, 22-24] is part of the procedure described in this paper. This method is based on the idea of determining the desired approximate value as an arithmetic mean of the upper and lower limits of the interval where the corresponding solution is expected to be. The COMSOL program package, based on the finite element method, is used to validate the results. The obtained results and the data analysis performed during validation suggest that the proposed, relatively simple approach is satisfactory accurate, especially for practical engineering purposes. There is no need for any integration involved in the procedure which reduces the resistance determination to an arithmetic equation. The proposed approach can also be extended to a hill modelled as a truncated cone consisting of three or more domains of different specific conductivity values. Also, the procedure can be used for both, flat or semi-spherically-shaped boundary surface between domains of different specific conductivity values.

2 Problem Description and Solution Procedure

2.1 Problem Description

The hemispherical ground electrode placed at the top of a hill approximated with a truncated cone is observed, as depicted in Figure 1. The cone consists of two homogeneous domains having specific conductivities σ_1 and σ_2. The radius of the electrode is r_0 and cone base radius is r_t. Other geometry parameters from Figure 1 are self-explanatory. In this paper, proposed solution for the structure from Figure 1 is based, as it has been already emphasized, on approaches from

[20] and [21]. However, the chosen model of non-homogeneous truncated cone is more complex and realistic structure related to those from [20] and [21]. One could expect that in general case ground structure is non-homogeneous and using the model from Figure 1 is a good way to take ground non-homogeneity into account.

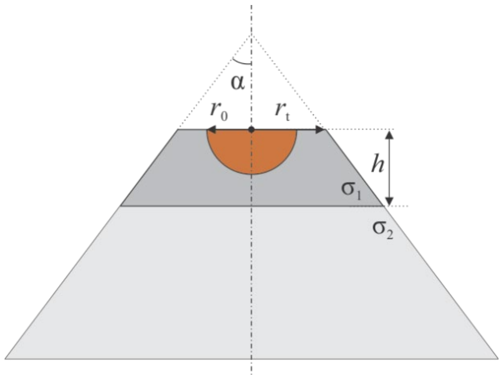

Figure 1
The hemispherical ground electrode at the top of a hill

2.2 Solution Procedure

Since approaches from [20] and [21] are the bases of solving of the problem illustrated in Figure 1, they will be briefly described in this chapter, before presentation of extended procedure applied on model from Figure 1.

2.2.1 Basic Procedure

In [20], the problem of hemispherical grounding electrode having radius r_0, placed at the top of the truncated homogeneous cone of a specific conductivity σ (Figure 2) is analysed and corresponding analytical solution for the low-frequency resistance is derived. A brief description of this procedure is given in this chapter.

The essence of the procedure given in [20] is approximation of the hemispherical electrode by a spherical sector of the radius R_1 (the center of spherical sector is at the fictitious peak of the cone), Figure 2. The parameters d and α are marked in the Figure 2. It is assumed that electrode is fed by the quasi-stationary current I.

From Figure 2 follows:

$$R_1 = r_0 + d\,,\ d = r_0 \cot\alpha \ \text{and}\ R_1 = r_0\left(1+\cot\alpha\right). \tag{1}$$

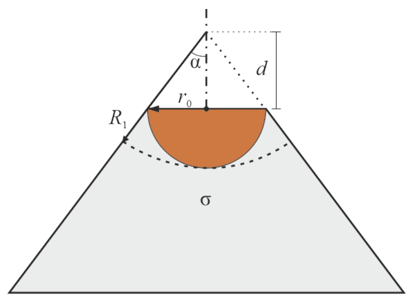

Figure 2
The hemispherical ground electrode at the top of a homogeneous truncated cone

A surface area of a spherical sector of radius R (coordinate orgin for this coordinate coincide with the fictitious pick of the cone) is $S = \Omega R^2$, where $\Omega = 2\pi(1-\cos\alpha)$ is solid angle. Hence, surface area is

$$S = R^2 2\pi(1-\cos\alpha). \tag{2}$$

Symmetry of the approximate geometry has as a consequence that current density depends only on radial coordinate r, i.e

$$\vec{J} = \frac{I}{S}\hat{R} = \frac{I}{R^2 2\pi(1-\cos\alpha)}\hat{r},\ R_1 < R < \infty. \tag{3}$$

Now, using the local form of Ohm's law, $\vec{J} = \sigma\vec{E}$, where $\vec{E}$ is electric field vector, the approximate potential of the electrode surface is

$$\varphi_s = \int_{R_1}^{\infty} \frac{J}{\sigma}\,\mathrm{d}R = \int_{R_1}^{\infty} \frac{I}{2\pi\sigma(1-\cos\alpha)R^2}\,\mathrm{d}R = \frac{I}{2\pi\sigma(1-\cos\alpha)R_1}. \tag{4}$$

Considering that $R_1 = r_0(1+\cot\alpha)$, the electrode surface potential is

$$\varphi_s = \frac{I}{2\pi\sigma(1-\cos\alpha)(1+\cot\alpha)r_0}. \tag{5}$$

Now, resistance of the hemispherical grounding electrode is

$$R_e = \frac{\varphi_s}{I} = \frac{I}{2\pi\sigma(1-\cos\alpha)(1+\cot\alpha)r_0}. \tag{6}$$

2.2.2 Improved Basic Procedure

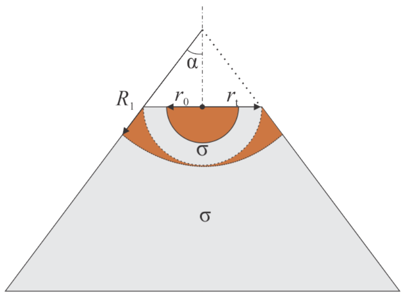

Figure 3
The hemispherical ground electrode at the top of a homogeneous truncated cone

The basic procedure from [20] is extended in [21] and applied to the problem of the hemispherical ground electrode having radius smaller than the radius of the cone basis, Figure 3. The electrode is fed in the center by quasi-stationary current I. The truncated cone has specific conductivity σ, while the radii of the hemispherical electrode and upper cone base are r_0 and r_t respectively ($r_0 < r_t$). This approach includes approximation of the current field with two different expressions.

Firstly, in area defined by $r_0 < r < r_t$, where r is radial coordinate having origin at the center of the hemispherical electrode, the current density vector is assumed as

$$\vec{J}_1 = \frac{I}{2\pi r^2}\hat{r},\; r_0 < r < r_t \,. \tag{7}$$

As in [20], a spherical sector of the radius R_1 (Figure 3) is introduced into the model. Below this sector, defined by $R_1 < R < \infty$, where R is radial coordinate having origin at the fictitious pick of the cone, for the current density vector the following expression is used

$$\vec{J}_2 = \frac{I}{2\pi\left(1-\cos\alpha\right)R^2}\hat{R},\; R_1 < R < \infty \tag{8}$$

Now, the potential of the electrode can be determined as

$$\varphi_s = \int_{r_0}^{r_t}\frac{J_1}{\sigma}\,\mathrm{d}r + \int_{R_1}^{\infty}\frac{J_2}{\sigma}\,\mathrm{d}R = \int_{r_0}^{r_t}\frac{I}{2\pi\sigma r^2}\,\mathrm{d}r + \int_{R_1}^{\infty}\frac{I}{2\pi\sigma\left(1-\cos\alpha\right)R^2}\,\mathrm{d}R \,. \tag{9}$$

From expression (9) follows

$$\varphi_s = \frac{1}{2\pi\sigma}\left[\frac{1}{r_0} - \frac{1}{r_t} + \frac{1}{(1-\cos\alpha)R_1}\right]. \tag{10}$$

Consenquently, the resistance of the hemispherical electrode from Figure 3 is

$$R_e = \frac{\varphi_s}{I} = \frac{1}{2\pi\sigma}\left[\frac{1}{r_0} - \frac{1}{r_t} + \frac{1}{(1-\cos\alpha)R_1}\right]. \tag{11}$$

2.2.3 Solution Procedure for the system from Figure 1

In order to approximately determine resistance of the hemispheric electrode from Figure 1, the model depicted in Figure 4 will be analysed. The truncated cone consists of two homogeneous domains having specific conductivities σ_1, i.e. σ_2. The electrode is fed by quasi-stationary current *I.* The radius of the electrode is r_0 and cone basis radius is r_t. The boundary surface between two domains is the spherical sector of the radius R_2.

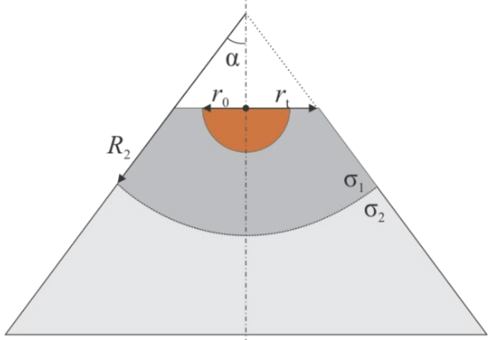

Figure 4
Hill approximated with two-domain truncated cone

A part of the system from Figure 4, consisting of hemispherical electrode and domain having specific conductivity value σ_1, is approximated as in [21] (and explained in 2.2.2), as it is shown in Figure 5. As proposed in [21], described part has been replaced with a hemispherical electrode placed in a shell with boundary of radius R_1. As already written, r_0 and r_t are the distances from the centre of the hemisphere, while R_1 and R_2 are distances from the origin positioned at the fictitious top of the cone. As in [21], the current field in a hemispherical shell around the electrode is assumed as radial, having a current density

$$\vec{J}_1 = \frac{I}{2\pi r^2}\hat{r},\ r_0 < r < r_t. \tag{12}$$

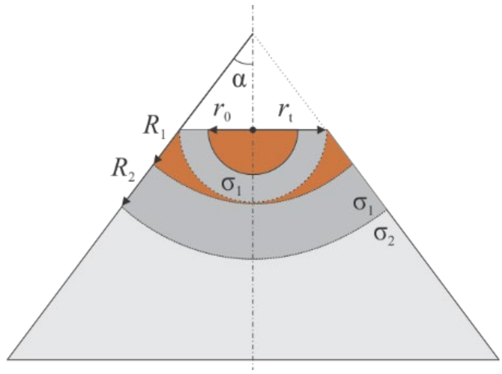

Figure 5
Illustration of the procedure from [21] for part of the system of specific conductivity σ_1

The current field in the rest of the domain of specific conductivity σ_1 is assumed as radial (following the approach from [21]), related to the fictitious top of the cone. It can be characterized by current density vector [21],

$$\vec{J}_2 = \frac{I}{2\pi\left(1-\cos\alpha\right)R^2}\hat{R},\ R_1 < R < R_2 . \tag{13}$$

In expression (13), R corresponds to the radial distance from the top of the cone, while $\hat{R}$ corresponds to radial ort. The same expression can also be applied for current density vector in the hill domain of specific conductivity σ_2 (defined with $R_2 < R < \infty$), based on the boundary condition for normal component of quasi-stationary current density vector, for $R = R_2$.

Now, the potential of the electrode surface related to the referent point placed on a large distance from the electrode, based on previous assumptions, can be determined as

$$\varphi_s = \int_{r_0}^{r_t} \frac{J_1}{\sigma_1}\mathrm{d}r + \int_{R_1}^{R_2} \frac{J_2}{\sigma_1}\mathrm{d}R + \int_{R_2}^{\infty} \frac{J_2}{\sigma_2}\mathrm{d}R . \tag{14}$$

In the previous expressions, dr and dR are differentials of the radial coordinates defined in the text above.

Now, using Ohm's law and equations (12)-(14), the following approximate expression for the electrode potential is obtained.

$$\varphi_s = \int_{r_0}^{r_t} \frac{I}{2\pi\sigma_1 r^2}\mathrm{d}r + \int_{R_1}^{R_2} \frac{I}{2\pi\sigma_1\left(1-\cos\alpha\right)R^2}\mathrm{d}R + \int_{R_2}^{\infty} \frac{I}{2\pi\sigma_1\left(1-\cos\alpha\right)R^2}\mathrm{d}R . \tag{15}$$

From (15), the resistance of the hemispherical electrode from Figure 3 is,

$$R_\mathrm{e} = \frac{\varphi_\mathrm{s}}{I} = \frac{1}{2\pi\sigma_1}\left\{\frac{1}{r_0} - \frac{1}{r_\mathrm{t}} + \frac{1}{(1-\cos\alpha)}\left[\frac{1}{R_1} - \frac{1}{R_2}\right]\right\} + \frac{1}{2\pi\sigma_2}\frac{1}{(1-\cos\alpha)R_2}. \tag{16}$$

where, from Figure 5 follows that

$$R_1 = (1+\cot\alpha)r_\mathrm{t}. \tag{17}$$

Finally, using equation (16) and the Estimation method [8, 22-24], it is possible to form an approximate expression for determining the ground electrode's resistance from Figure 1. In Figure 6 are labelled upper (R_{2e}) and lower (R_{2i}) values of boundary surface radii. The approximate resistance of the system is determined as arithmetic mean of the resistance values obtained for Figure 6,

$$R_{2i} = (1+\cot\alpha)r_\mathrm{t} \text{ and } R_{2e} = \frac{h + r_\mathrm{t}\cot\alpha}{\cos\alpha}. \tag{18}$$

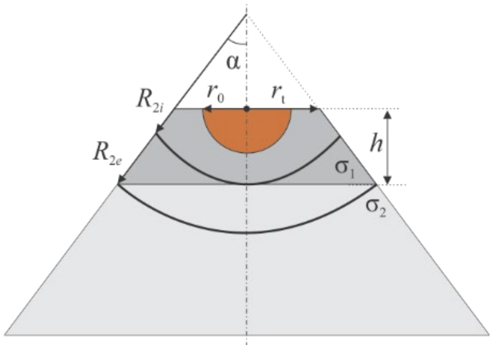

Figure 6
Estimation method application

Now, for $R_2 = R_{2i}$ the value of the electrode resistance $R_\mathrm{e} = R_{\mathrm{e}i}$ is

$$R_{\mathrm{e}i} = \frac{1}{2\pi\sigma_1}\left\{\frac{1}{r_0} - \frac{1}{r_\mathrm{t}} + \frac{1}{(1-\cos\alpha)}\left[\frac{1}{R_1} - \frac{1}{R_{2i}}\right]\right\} + \frac{1}{2\pi\sigma_2}\frac{1}{(1-\cos\alpha)R_{2i}}. \tag{19}$$

For $R_2 = R_{2e}$ obtains electrode resistance $R_\mathrm{e} = R_{\mathrm{e}e}$, i.e.

$$R_{\mathrm{e}e} = \frac{1}{2\pi\sigma_1}\left\{\frac{1}{r_0} - \frac{1}{r_\mathrm{t}} + \frac{1}{(1-\cos\alpha)}\left[\frac{1}{R_1} - \frac{1}{R_{2e}}\right]\right\} + \frac{1}{2\pi\sigma_2}\frac{1}{(1-\cos\alpha)R_{2e}}. \tag{20}$$

The approximate resistance value is obtained as the mean value of R_{2i} and R_{2e}

$$R_{e\,ap} = \frac{R_{ei} + R_{ee}}{2}, \text{ i.e.} \tag{21}$$

$$R_{e\,ap} = \frac{1}{2\pi\sigma_1}\left\{\frac{1}{r_0} - \frac{1}{r_t} + \frac{1}{(1-\cos\alpha)}\left[\frac{1}{R_1} - \frac{R_{2e}+R_{2i}}{2R_{2e}R_i}\right]\right\} + \\ + \frac{1}{2\pi\sigma_2(1-\cos\alpha)}\frac{R_{2e}+R_{2i}}{2R_{2e}R_i}. \tag{22}$$

3 Results

The described method is applied for $\sigma_1 = 0.01\,\mathrm{S/m}$ and $r_0 = 5\,\mathrm{m}$, while the rest of the parameters from Figure 1 take the following values: $\alpha \in \{45^0, 50^0, 55^0, 60^0\}$, $r_t \in \{5\,\mathrm{m}, 10\,\mathrm{m}, 15\,\mathrm{m}\}$, $h \in \{5\,\mathrm{m}, 10\,\mathrm{m}\}$ and $\sigma_2/\sigma_1 \in \{0.5, 5\}$. The values of the parameters have been selected based on [20]-[22]. The obtained results ($R_{e\,ap}$) are validated with the values obtained from the COMSOL program package application (R_e). Number of boundary elements used during the simulation is 18562, while total number of elements is 308473. Electric potential distribution obtained in COMSOL for α=45^0, r_0=5 m, r_t=10 m, h=20 m, σ_1=0.01 S/m and σ_2=0.0001 S/m is shown in Figure 7.

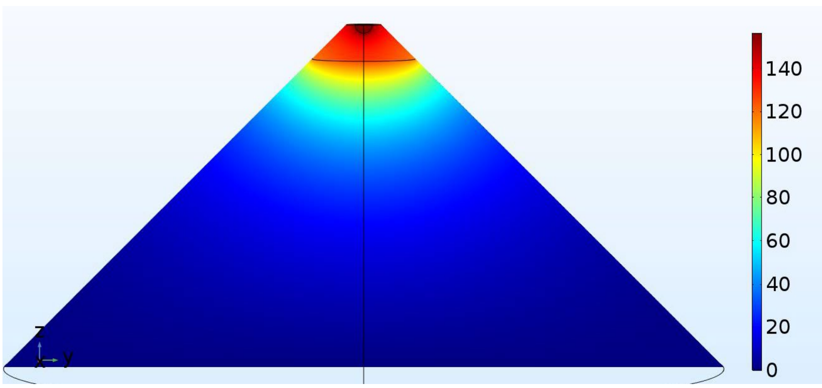

Figure 7

Electric potential distribution for α=45^0, r_0=5 m, r_t=10 m, h=20 m, σ_1=0.01 S/m and σ_2=0.0001 S/m

The results ($R_{e\,ap}$, R_e and relative error) for $\alpha \in \{45^0, 50^0, 55^0, 60^0\}$ are given in Tables 1-4, respectively. Graphics shown in Figures 8-11 correspond to Tables 1-4 respectively and contain relative error versus angle α value.

The maximum deviation of the presented results (Tables 1-4) is 15.7%, while the standard deviation value is 4.541% (based on the results from Tables 1-4), related to the median value of 5.001%.

Table 1

The results for $\alpha=45^0$

r_t[m]	h[m]	σ_2 / σ_1	$R_{e\,ap}$ [Ω]	R_e[Ω]	Relative error [%]
5	10	0.5	85.260	86.979	1.977046
		5	29.602	35.110	15.68705
	20	0.5	72.891	74.731	2.461634
		5	39.497	45.459	13.1162
10	10	0.5	66.276	65.490	1.199309
		5	24.532	26.905	8.816484
	20	0.5	58.545	57.621	1.60396
		5	30.717	33.770	9.040823
15	10	0.5	57.886	56.317	2.785968
		5	24.492	25.113	2.47417
	20	0.5	52.585	50.564	3.9976
		5	28.732	30.455	5.657585

Table 2

The results for $\alpha=50^0$

r_t[m]	h[m]	σ_2 / σ_1	$R_{e\,ap}$ [Ω]	R_e[Ω]	Relative error [%]
5	10	0.5	74.233	76.341	2.761091
		5	27.828	32.805	15.16972
	20	0.5	63.578	65.790	3.361815
		5	36.352	41.843	13.12202
10	10	0.5	60.041	59.690	0.589018
		5	24.222	26.182	7.485269
	20	0.5	53.032	52.567	0.885395
		5	29.830	32.524	8.284733
15	10	0.5	53.575	52.558	1.934003
		5	24.409	24.754	1.3937
	20	0.5	48.602	47.136	3.110419
		5	28.387	29.880	4.99731

Table 3

The results for $\alpha=55^0$

r_t[m]	h[m]	σ_2 / σ_1	$R_{e\,ap}$ [Ω]	R_e[Ω]	Relative error [%]
5	10	0.5	65.655	67.773	3.125576
		5	26.504	30.907	14.2475
	20	0.5	56.400	58.725	3.95919

		5	33.908	38.896	12.82292
10	10	0.5	55.139	54.986	0.278231
		5	24.050	25.599	6.04808
	20	0.5	48.743	48.520	0.459313
		5	29.167	31.494	7.387051
15	10	0.5	50.178	49.445	1.48177
		5	24.397	24.470	0.295781
	20	0.5	45.482	44.358	2.535321
		5	28.154	29.398	4.233505

Table 4
The results for $\alpha=60^0$

r_t[m]	h[m]	σ_2 / σ_1	$R_{e\,ap}$ [Ω]	R_e[Ω]	Relative error [%]
5	10	0.5	58.885	60.850	3.228145
		5	25.540	29.320	12.89244
	20	0.5	50.791	53.017	4.19838
		5	32.015	36.424	12.10466
10	10	0.5	51.231	51.113	0.229494
		5	23.988	25.124	4.522457
	20	0.5	45.358	45.223	0.299508
		5	28.685	30.641	6.383074
15	10	0.5	47.468	46.885	1.243428
		5	24.439	24.241	0.815542
	20	0.5	43.004	42.071	2.216863
		5	28.010	29.004	3.427549

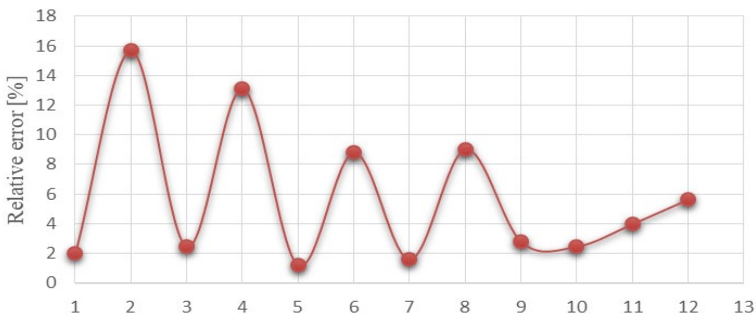

Figure 8
Relative error for different samples when $\alpha=45^0$ (Table 1)

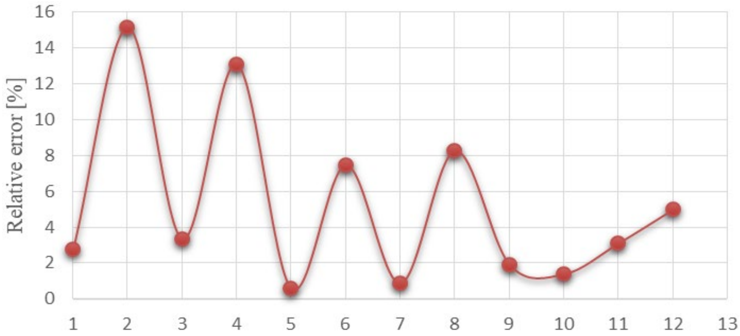

Figure 9
Relative error for different samples when $\alpha=50^0$ (Table 2)

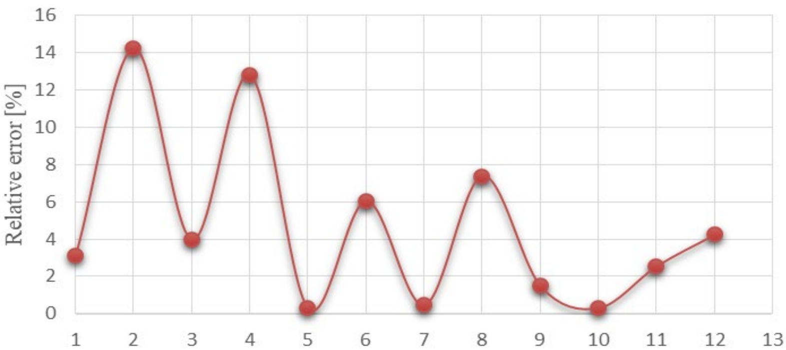

Figure 10
Relative error for different samples when $\alpha=55^0$ (Table 3)

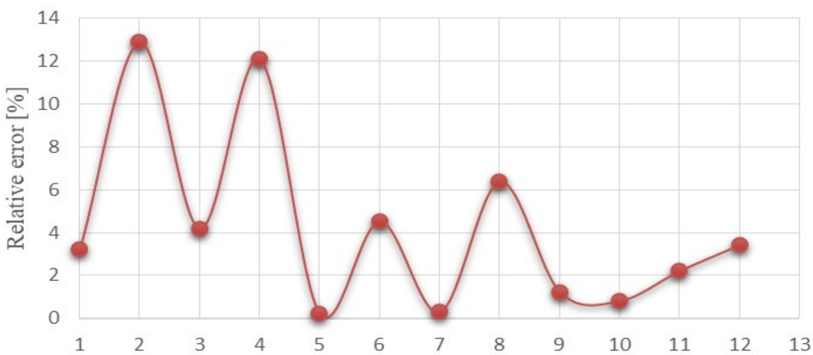

Figure 11
Relative error for different samples when $\alpha=60^0$ (Table 4)

Discussion and Conclusions

An approximate analytical procedure for determining the resistance of a hemispherical electrode, placed on top of a mountain, is presented. The mountain is modelled as truncated cone with two domains. Proposed procedure is a kind of extension of the methods given in [20] and [21]. Based on the obtained results, it can be concluded that the proposed approach is satisfactorily accurate, especially for engineering applications. The method does not involve any type of integration and reduces resistance determination to a simple arithmetic equation. It can also be extended to a hill modelled as a truncated cone consisting of three or more domains of different specific conductivity values.

Acknowledgement

This work has been supported by the Ministry Science, Technological Development and Innovation of the Republic of Serbia.

References

[1] T. Takashima, T. Nakae, R. Ishibahsi: High frequency characteristics of impedances to ground and field distributions of ground electrodes, IEEE Transaction on Power Apparatus and Systems, 1980, 100, pp. 1893-1900

[2] R. J. Heppe: Step potential and body currents near grounds in two-layer earth, IEEE Transactions on Power Apparatus and Systems, 1979, 98, pp. 45-59

[3] P. D. Rancic, L. V. Stefanovic, Dj. R. Djordjevic: A new model of the vertical ground rod in two-layer earth, IEEE Transaction on Magnetics, 1992, 28, pp. 1497-1500

[4] P. D. Rancic, L. V. Stefanovic, Dj. R. Djordjevic: An improved linear grounding system analysis in two-layer earth, IEEE Transaction on Magnetics, 1995, 32, pp. 5179-5187

[5] P. D. Rancic, Z. P. Stajic, Dj. R. Djordjevic, B. S. Tosic: Analysis of linear ground electrodes plaed in vertical three-layer earth, IEEE Transaction on Magnetics, 1996, 32, pp. 1505-1508

[6] N. N. Cvetkovic, P. D. Rancic: A simple model for a numerical determination of electrical characteristics of a pillar foundation grounding system, Engineering Analysis with Boundary Elements, Elsevier, 2009, 33, pp. 555-560

[7] N. N. Cvetkovic, P. D. Rancic: Influence of foundation on pillar grounding system's characteristics, COMPEL: The International Journal for Computation and Mathematics in Electrical and Electronic Engineering, 2009, 28, pp. 471-492

[8] D. D. Vuckovic, N. N. Cvetkovic, M. S. Stojanovic, I. Iatcheva: Approximate model for ground inhomogeneity with rectangular cross-

section: application to analysis of grounding systems. Electrical Engineering, 2018, 100, pp. 75-82

[9] C. Andreeski, D. Mechkaroska: Modelling, forecasting and testing decisions for seasonal time series in tourism, Acta Polytechnica Hungarica, 2020, 17, pp. 149-171

[10] Elena-Lorena Hedrea, Radu-Emil Precup, Raul-Cristian Roman, Emil M. Petriu: Tensor product-based model transformation approach to tower crane systems modeling, Asian Journal of Control, 2021, 23, pp. 1313-1323

[11] C. J. Kwak, K.-C. Ri, S.-I. Kwak, K.-J. Kim, U.-S. Ryu, O.-C. Kwon, N.-H. Kim: Fuzzy modus ponens and tollens based on moving distance in SISO fuzzy system, Romanian Journal of Information Science and Technology, 2021, 24, pp. 257-283

[12] N. Yapici Pehlivan, I. B. Turksen: A novel multiplicative fuzzy regression function with a multiplicative fuzzy clustering algorithm, Romanian Journal of Information Science and Technology, 2021, 24, pp. 79-98

[13] I.-D. Borleaa, R.-E. Precup, A.-B. Borlea: Improvement of K-means cluster quality by post processing resulted clusters, Procedia Computer Science, 2022, 199, pp. 63-70

[14] A.-I. Szedlak-Stineana, R.-E. Precup, E. M. Petriu, R.-C. Roman, E.-L. Hedrea, C.-A. Bojan-Dragos: Extended Kalman filter and Takagi-Sugeno fuzzy observer for a strip winding system, Expert Systems with Applications, 2022, 208, 118215

[15] D. Poljak: Advanced Modeling in Computational Electromagnetic Compatibility; Wiley-Interscience: NJ, USA, 2007

[16] F. Rachidi, M. Rubinstein, A. Smorgonskiy: Lightning Protection of Large Wind-Turbine Blades. In Wind Energy Conversion Systems; S. Muyeen, Eds.; Springer: London, UK, 2012

[17] A. Smorgonskiy, F. Rachidi, M. Rubinstein, G. Diendorfer: On the relation between lightning flash density and terrain elevation. In Proceedings of the International Symposium on Lightning Protection, Belo Horizonte, Brazil, 7-11 October 2013

[18] J. Montanyà, O. Van der Velde, E. R. Willians: Lightning discharges produced by wind turbines, Journal of Geophysical Research Atmospheres, 2014, 119, pp. 1455-1462

[19] L. D. Grcev, A. Kuhar, V. Arnautovski-Toseva, B. Markovski: Evaluation of high-frequency circuit models for horizontal and vertical grounding electrodes, IEEE Transactions on Power Delivery, 2018, 33, pp. 3065-3074

[20] A. Sunjerga, F. Rachidi, M. Rubinstein, D. Poljak: Calculation of the grounding resistance of structures located on elevated terrain, IEEE Transactions on Electromagnetic Compatibility, 2019, 61, pp. 1891-1895

[21] K. B. Tan, H. M. Lu, Y. Zhang, W. C. Zuo: Analysis of the grounding resistance of a hemispheric electrode located on a truncated cone, IEEE Transactions on Electromagnetic Compatibility, 2020, 62, pp. 1361-1363

[22] N. N. Cvetkovic, P. D. Rancic: Model for analyzing a pillar grounding system with cylindrically-shaped concrete foundation, Electromagnetics, 2009, 29, pp. 151-164

[23] P. D. Rancic, N. N. Cvetkovic: Square shaped electrode as pillar grounding system, 9th International Conference on Telecomunications in Modern Satellite, Cable and Broadcasting Services-TELSIKS 2009, October 07-09, 2009, Nis, Serbia, Proceeding of papers, Volume 2, pp. 351-354

[24] N. N. Cvetkovic, D. D. Vuckovic, M. Stojanovic, D. Krstic, D. Tasic: The grounding system of the pillar on the road, 11th International Conference on Telecomunications in Modern Satellite, Cable and Broadcasting Services-TELSIKS 2013, October 16-19, 2013, Nis, Serbia, CD Proceedings pp. 45-48